LAWRENCE
LIVERMORE
NATIONAL
LABORATORY

LLNL-JRNL-645860

Ka and bremsstrahlung x-ray radiation backlighter sources from short pulse laser driven silver targets as a function of laser pre-pulse energy

A. G MacPhee, L. C. Jarrptt, A. Kemp, L. Divol, D. Mariscal, B. Westover, C. McGuffey, F. Beg, M. Suggit, C. Chen, D. Hey, B. Maddox, J. Hawreliak, H. Park, B. Remington, M. S. Wei

November 7, 2013

Physics of Plasmas

Disclaimer

This document was prepared as an account of work sponsored by an agency of the United States government. Neither the United States government nor Lawrence Livermore National Security, LLC, nor any of their employees makes any warranty, expressed or implied, or assumes any legal liability or responsibility for the accuracy, completeness, or usefulness of any information, apparatus, product, or process disclosed, or represents that its use would not infringe privately owned rights. Reference herein to any specific commercial product, process, or service by trade name, trademark, manufacturer, or otherwise does not necessarily constitute or imply its endorsement, recommendation, or favoring by the United States government or Lawrence Livermore National Security, LLC. The views and opinions of authors expressed herein do not necessarily state or reflect those of the United States government or Lawrence Livermore National Security, LLC, and shall not be used for advertising or product endorsement purposes.

Kα and bremsstrahlung x-ray radiation backlighter sources from short pulse laser driven silver targets as a function of laser pre-pulse energy

L.C. Jarrott[1], A. J. Kemp[2], L. Divol[2], D. Mariscal[1], B. Westover[1,2], C. McGuffey[1], F.N. Beg[1], M. Suggit[3], C. Chen[2], D. Hey[2], B. Maddox[2], J. Hawreliak[2], H.-S. Park[2], B. Remington[2], M.S. Wei[4] and A. MacPhee[2]

[1]*Center for Energy Research, University of California San Diego, La Jolla, CA 92093*
[2]*Lawrence Livermore National Laboratory, Livermore, CA 94550*
[3]*Department of Physics, Clarendon Laboratory, University of Oxford, Oxford, OX1 3PU, UK*
[4]*General Atomics, P.O. Box 85608, San Diego, CA92186-5608*

Abstract

Measurements of silver K-shell and bremsstrahlung emission from thin-foil laser targets as a function of laser prepulse energy are presented. The silver targets were chosen as a potential 22 keV backlighter source for the National Ignition Facility Experiments. The targets were irradiated by the Titan laser with an intensity of 8×10^{17} W/cm^2 with 40 ps pulse length. A secondary nanosecond timescale laser pulse with controlled, variable energy was used to emulate the laser prepulse. Results show a decrease in both K_α and bremsstrahlung yield with increasing artificial prepulse. Radiation hydrodynamic modeling of the prepulse interaction determined that the preplasma and intact target fraction were different in the three prepulse energies investigated. Interaction of the short pulse laser with the resulting preplasma and target were then modeled using a Particle-In-Cell code PSC which explained the experimental results. The relevance of this work to future Advanced Radiography Capability x-ray backlighter sources is discussed.

I. Introduction

High energy, monoenergetic laser-produced photon sources have many applications in diagnosing inertial confinement fusion (ICF) plasmas[1-3] and other high energy-density plasma (HEDP) systems[4-8]. To produce these sources, a short duration, high intensity laser pulse interacts with a metallic foil target. Electrons from the metallic foil are then accelerated within the electric and magnetic fields of the laser to relativistic velocities. These "fast" electrons make binary collisions inside the target and emit K_α and bremsstrahlung radiation. The line emission from the K-shell of the metallic foil can then be used as a high-energy monochromatic photon source with short pulse duration for the radiography of very dense materials[9,10]. Additionally, the target itself is a high-energy density system and details of these emissions help to diagnose the system as described in this paper.

Previous work has shown high intensity short-pulse produced K-shell line emission to be a very effective radiography source[1,8-13]. In previous experiments[9], optimization of the backlighter target geometry led to high-resolution and high conversion efficiency from laser energy to K_α photons. High contrast (10^{-10}) lasers have been used[8] to show significant enhancements in total K_α for both Mo and Ag targets. Higher conversion efficiencies are due, in part, to the electrostatic potential buildup on the target preventing a large fraction of accelerated electrons from leaving the target, and instead forcing them to make multiple passes (reflux) through the target until all of their energy is given to the target. Previous work[11] has shown

dependence of K_α yield on laser intensity and pulse length as well as shown further verification of electrostatic fields surrounding the target causing refluxing and hence, K_α enhancement. In other experiments[6], high intensity laser produced tungsten K_α is used as a backlighter source for measuring the density in shocked and unshocked iron to deduce the equation of state (EOS) at high-density and high-pressure. Here the signal to noise of the backlighter is critical for making accurate measurements of the density and hence EOS. However, there is no systematic study yet according to our knowledge on the effect of joule level laser prepulse inherent to high intensity short pulse lasers on the brightness of these high energy radiation sources. Particularly, it is important to determine the tolerable laser prepulse for radiography sources using Advance Radiography Capability laser (ARC) at the Lawrence Livermore National Laboratory.

In this paper, we discuss the effects of laser prepulse energy on the conversion efficiency of laser energy to K_α photons from silver foil targets. Measurements of K_α photons, bremsstrahlung and escaping electrons were measured while varying the laser prepulse energy over two orders of magnitude (50 mJ up to 5 J) to infer a scaling with prepulse level. This is an important regime to investigate in advance of future multi-kilojoule laser facilities such as the Advance Radiography Capability laser[14] at the National Ignition Facility. Simulations were also carried out to model the hydrodynamics of target expansion due to the prepulse as well as for the electron source and transport of fast electrons within the target.

The paper is structured as follows: Section II describes the experimental setup and data analysis methods; Section III describes the experimental results; Section IV describes modeling methods and results; Section V discusses the implications of both experimental and modeling results and summarizes.

II. Experimental Setup and Diagnostics

The experiment was carried out using the Titan laser at the Jupiter Laser Facility in Lawrence Livermore National Laboratory. Targets were silver foils, 12µm thick and 250µm diameter. They were irradiated by a 1.050µm wavelength laser at an angle of 16 degrees with respect to target normal, in a 30µm diameter spot with a Full-width at Half Maximum (FWHM) pulse duration of 40ps and total energy of 300J, resulting in a laser intensity of 8×10^{17} W/cm^2. In addition, a long pulse (3ns), 1.053µm wavelength laser was injected coaxially with the short pulse beam as a means to artificially increase prepulse energy beyond the nominal 15mJ due to amplified spontaneous emission (ASE) inherent to the short pulse. The delay between the arrival of the long pulse and the short pulse was set at 3ns, similar to the typical ASE pedestal pulse duration from the short pulse beam. The long pulse parameters had a slightly larger focal spot diameter of 50µm, and energy was varied from 50mJ to 5000mJ. With this, the resulting power contrast ratio for this experiment ranged from 10^{-6} to 10^{-4} while the energy contrast ranged from 10^{-4} to 10^{-2}.

Silver K_α at 22keV and high-energy bremsstrahlung x-rays produced from the interaction of these targets with both the Titan short and long pulses were measured using several independent diagnostics listed below. Experimental layout is shown in Fig. 1.

i) A Highly Ordered Pyrolytic Graphite spectrometer (HOPG)[15] placed at 80° with respect to rear side target normal was used to measure x-rays in the range of 20 to 24 keV including the K_α line of silver.

ii) A Transmission Crystal Spectrometer (TCS)[16] placed at 80° with respect to front side target normal was used in conjunction with the HOPG to confirm silver K_α yield. Integrated

yield output from both HOPG and TCS are given in units of photostimulated luminescence (PSL).

iii) A single hit CCD (SH-CCD)[17] was run concurrently on all shots to calibrate the integrated Ag K_α yields of i) and ii) from PSL to absolute photon numbers.

iv) Two hard x-ray bremsstrahlung spectrometers (HXBS) were placed on the front and rear side of target normal to measure the fast electron-produced bremsstrahlung from within the target. Differences between the front and rear side yield results could be used to examine the effects of refluxing. The HXBS consists of 15 imaging plates stacked in series with filter materials of increasing Z and/or thickness placed in front of each imaging plate starting with 100μm of aluminum in front of the first and ending with 6mm of lead in front of the last imaging plate. The details of this diagnostic can be found elsewhere[2]. This diagnostic provides a spectral range from roughly 12keV to 700keV. In this design, high-energy bremsstrahlung photons deposit their energy on the imaging plates in varying doses depending on the photon energy and the cumulative filtering by the preceding layers. Self-emission from the interaction of the high energy primary photons with the filters within the diagnostic also contribute to signal on the imaging plates.

The response of the diagnostic stack, including self-emission, was determined using 1D photon transport simulations of the diagnostic with the Monte Carlo electron/photon transport code INTEGRATED TIGER SERIES 3.0 (ITS)[18]. The ITS simulation consisted of modeling the expected energy deposition on each imaging plate by individually propagating 151 logarithmically spaced monoenergetic photon beams ranging from 1keV to 100MeV through the diagnostic. ITS was also used to simulate the bremsstrahlung response of the target by propagating a beam of electrons through the silver target for 81 logarithmically spaced monoenergetic electron beams ranging from 10keV to 100MeV. Parameterizing the 81 monoenergetic electron beams by assuming a Boltzmann distribution of electrons, the bremsstrahlung distribution predicted by the target response was calculated. The distribution was used to calculate the expected energy deposition on the imaging plates which was then compared with the experimental data. This process was iterated with the Boltzmann temperature, laser-to-electron conversion efficiency, and electron source divergence as free parameters until the predicted energy deposition matched well to the deposited energy on the imaging plates from the experimental data.

v) A vacuum electron spectrometer (ESPEC)[19] was placed at rear side target normal and used to measure fast electrons that escaped the target. The ESPEC consists of a ~0.5T magnet placed ~1m from target chamber center which deflects electrons with energy up 100MeV onto an imaging plate. Lower energy electrons are more preferentially deflected by the magnet and so the resulting signal on the imaging plate is an energy spectrum of escaping electrons. This diagnostic is absolutely calibrated and so the total number of electrons can be inferred from the signal on the imaging plate in addition to Boltzmann-like steady-state “slope” temperatures.

III. Experimental Results

Integrated K_α yields for the HOPG and TCS are plotted as a function of prepulse energy in Fig. 2. Both the HOPG and TCS agreed to within 1% of one another for all shots taken throughout this experiment. Although the HOPG and TCS were on opposite sides of the target, this agreement was expected as K_α is produced from collisions with fast electrons and K-shell electrons and is emitted isotropically in our thin foil targets. In this scan, three different prepulse

energies were used, 50mJ, 500mJ, and 5000mJ. Results show decreasing K_α yield by a factor of 4 when the prepulse energy was increased by 2 orders of magnitude. Calibration of the HOPG and TCS diagnostics with the SH-CCD show absolute photon numbers in the range of $3x10^{11}$ to $1x10^{12}$ photons/sr. With mass-limited targets and intensities at 10^{18} W/cm^2, previous work[20] showed that the majority of fast electrons produced (as much as 99%) experienced refluxing with the majority of their energy being deposited back into the target through direct collisions with ions and with background electrons.

The HXBS diagnostic was analyzed following the methodology described in Sec. II and detailed in a previous work[2]. The resulting inferred bremsstrahlung spectrum is plotted in Fig. 3 as a function of increasing prepulse energy. Here, the K and L edges (25.5keV and 3.4 – 3.8keV) are visible in all 3 spectra. They are then integrated over energy to get the total energy of the bremsstrahlung radiation produced, listed inset. The inferred bremsstrahlung results show a similar trend to the K_α yield detected by the HOPG and TCS as seen in Fig. 2: the total integrated bremsstrahlung energy decreased by slightly more than a factor of 3 when increasing the prepulse by 2 orders of magnitude. The total number of photons produced in the range of 1 keV to 100 MeV is of the order 10^{12} photons/sr. The calculated K_α yield from the ITS analysis process, discussed in more detail in the next section, is also shown in Fig. 2 and is consistent with that measured by the HOPG and TCS diagnostics.

Compared to K_α emission, bremsstrahlung emission directionality is more strongly dependent on the directionality of the fast electrons. By measuring the bremsstrahlung on both the front and rear side of the target, refluxing, as described in previous work[20] and discussed extensively in the literature[9-11,20], could be verified. Bremsstrahlung incident on the front side detector is due, in large part to refluxing[11]. Previous simulations[11] for both refluxing and non-refluxing cases were done. The results of that study showed the ratio of rear side to front side bremsstrahlung energy to be 2 for the non-refluxing case and 1.3 for the refluxing case. Here, results from the two bremsstrahlung spectrometers show a ratio of 1.2 for the 50mJ prepulse energy and increasing up to 1.4 for the highest (5000mJ) prepulse energy. This increase in the ratio (rear to front side) of the total integrated bremsstrahlung energy demonstrates a slight diminishing in the refluxing efficiency as the prepulse energy was increased by 2 orders of magnitude. As discussed previously[11], refluxing allows for multiple passes of electrons, which in turn gives higher yields for both K_α and bremsstrahlung. In this particular case, the reduction in inferred refluxing is relatively small when compared to the factor of 4 reduction in K_α meaning this mechanism cannot be the only explanation for the experimentally observed K_α signal reduction.

Fig. 4 shows escaping electron spectrum as measured by the ESPEC. Results show an *increase* in escaping electron number and energy with increasing prepulse, which has been seen in previous studies[22-24] involving large pre-formed plasmas. Total energy in escaping electrons increases by roughly a factor of 3 from 0.6J to 1.8J when increasing the prepulse energy by 2 orders of magnitude. More energy in the form of fast electrons escaping the target results in less energy from fast electrons being deposited back into the target via refluxing which in turn means reduction in K_α signal. Similar to the HXBS, the ESPEC shows an inferred reduction in refluxing, although not large enough to explain the entirety of the K_α reduction seen on the HOPG and TCS.

IV. Modeling Methods, Results and Discussion

The experimental data needs modeling validation to determine the cause of the reduction in both K_α and bremsstrahlung yields. The change in prepulse level will change both the interaction region of the laser as well as the transport region within the target. Changes to the electron source due to changing underdense preplasma conditions as well as reduced solid density regions with a prepulse as high as 5000mJ will greatly affect laser to electron conversion efficiency and K_α production efficiency, respectively. Many effects contribute to the overall coupling of laser energy into K_α photons including LPI, target ablation, fast electron transport, and K_α cross-section as a function of electron energy.

To include these effects in our interpretation of the data, a variety of codes including HYDRA[25], ITS[18], and PSC[26] were used to simulate various aspects of the experiment. These simulations helped to determine roles of each of the various mechanism played in reducing the K_α and bremsstrahlung signals while simultaneously increasing the number of escaping electrons. The high energy prepulse creates a large (10's of microns) preformed plasma which significantly changes the interaction region of the short pulse beam; it also ablates away a significant amount (as little as 40% remaining) of the 12µm thick silver target and therefore also changes the transport region of the fast electrons. To confirm this, the radiation hydrodynamic simulations were carried out using HYDRA to determine the extent of the preplasma produced for all three prepulse levels. The final electron density lineouts after 3ns of prepulse are plotted in Fig. 5. Results show 2µm of the target being ablated away for a 50mJ prepulse and the critical density extending to 3µm in front of the solid target surface at the arrival time of the short pulse beam. For the 500mJ prepulse case, roughly 4µm of target is ablated away and the critical density is extended to 12µm from the target. In the most extreme 5000mJ prepulse case, 7µm of the target is ablated away from the target leaving only 5µm of solid-density target. In this case the critical density extended to 27µm, which drastically changes the transport region for the fast electrons.

Although the HXBS records all x-rays from 12keV to 700keV, the results can be compared with target simulations done using ITS which can then infer the predicted K_α yield that would result from the recorded bremsstrahlung emission which can then be compared with experimental K_α yield results from both the HOPG and TCS. The ITS target simulations were carried out using the predicted remaining solid target from the HYDRA simulations to better represent the number of remaining solid silver atoms capable of efficiently producing silver K_α. Given that only one HXBS was fielded on each side of the target, the predicted electron source divergence had a very large uncertainty. To determine the sensitivity of the inferred results on divergence, multiple ITS simulations were carried out with a range of electron divergences scaling from 40 to 80 degree half angle, which covers the range previously observed from experiments on the laser system[2,3,11]. The results were then averaged with the error bars consisting of the imaging plate error and the standard deviation of the different source divergence simulations, combined in quadrature. It is this predicted K_α yield that is plotted along with the HOPG and TCS results in Fig. 2 which agree to within one standard deviation.

ITS has been used previously[11] to infer laser to electron conversion efficiency by analyzing in conjunction with the HXBS data; but the results will be overestimated with this target geometry due to the fact that the production of both K_α and bremsstrahlung comes from fast electrons making multiple passes through the target while these specific ITS target simulations only account for one pass. Because of this, a more sophisticated code, PSC was used to simulate the laser-plasma interaction and infer relative conversion efficiencies.

In order to validate the experimental results and deconvolve the issue of reduced fast electron interaction with the target with increasing prepulse, the particle-in-cell code PSC (1D) was used with the HYDRA preplasma profiles to simulate the electron source for each prepulse case which was then compared to the ITS fitting calculations to validate experimental K_α and bremsstrahlung information. The intensity used for all three cases was matched to the experimental values at $8x10^{17}$ W/cm^2. Fig. 6 shows the 1D PSC electron source spectrum, sampled from a "box" behind the critical density over a depth of 50µm. Results show that relative conversion efficiency from laser to fast electrons entering the solid target with energy greater than 22keV decreases by a factor 3 as the prepulse energy is increased from 50mJ to 5000mJ.

V. Discussion

To compare the results from the PSC simulations with K_α yield measurements, we assume a highly refluxing regime[20]. With a predominately refluxing population of fast electrons, fast electron energy deposition and observed K_α yield are highly correlated because most electrons will lose all of their energy into the target. To get a rough estimation of electron energy deposition, ESTAR stopping power coupled with the areal density from HYDRA was used for each electron energy bin from the PSC simulations. Assuming, hypothetically, that the number of K_α photons is proportional to the *total* deposited energy from *all* electrons with energy greater than the silver K_α line energy (22keV), the energy deposition would decrease linearly with laser-to-electron conversion efficiency. Taking the relative conversion efficiencies from the PSC simulations for each pre-pulse case, we would expect a decrease in K_α yield by a factor of 3, which is slightly less than the decrease observed in experiment. However, the assumption that all electrons above 22keV deposit their energy into the target and result in silver K_α emission is an obvious overestimate. As stated previously, HXBS results showed an increase in the ratio of the target rear side to front side integrated bremsstrahlung energy as the laser prepulse was increased. This change is attributable to a reduction in electron refluxing in the target. With less radiated energy due to refluxing electrons, as seen by the HXBS for the 5000mJ prepulse case, one would expect less energy deposition into the target by fast electrons and therefore fewer silver K_α photons. This is consistent with the fact that the PSC simulation infers a K_α yield reduction factor of only 3, assuming a linear scaling of K_α with fast electron energy deposition, while the experimental measurements give a factor of 4. Comparison of the normalized fast electron energy deposition into the target from PSC is plotted along with integrated HOPG yield in Fig. 7.

In addition to the reduction in refluxing seen by the HXBS with increasing prepulse, the escaped electron spectra seen by the ESPEC also showed an *increase* in the total number and energy of electrons that escaped the target. This can be seen when integrating the total energy in escaped electrons and also in the strong reduction in the low energy component electron sprectra in the 50mJ pre-pulse case. Compound that with the results from PSC showing a reduction in conversion efficiency means that the fraction of electrons that escape the target *without* refluxing must have increased with increasing prepulse. Utilizing a maximum estimated experimental conversion efficiency of 30% from previous work[11], where the laser and target parameters were very similar, we can deduce from the relative reduction in conversion efficiency seen in the PSC simulations that the conversion efficiency for the 5000mJ prepulse could not be more that 10%. With a 300J laser, that leaves 30J of energy converted to fast electron kinetic energy. The

ESPEC showed 1.78J in escaping electron energy which corresponds to 6% of the total electron energy that does not contribute to refluxing. That is up from 0.6% of the fast electron energy escaping in the 50mJ prepulse case. Both the HXBS and the ESPEC show a reduction in refluxing with the HXBS seeing an enhancement in rear to front side bremsstrahlung energy ratio from 1.2 to 1.4 and the ESPEC seeing roughly 6% of fast electrons escaping the target.

From this, the dominant mechanism for reduction in K_α yield with increasing prepulse is the conversion efficiency of laser energy into fast electrons. A secondary mechanism apparent in both the HXBS and ESPEC is the reduction in refluxing efficiency causing less fast electron energy to be deposited into the target. A tertiary explanation for the slight disagreement between the PSC relative reduction in conversion efficiency and the experimentally seen reduction in K_α yield could be due to the fact the simulations are one dimensional meaning the relative importance of multi dimensional effects such as laser defocusing and self-generated fields are not properly represented. Results for both simulation and experiment show good agreement in this regard.

In summary, this study is the first to measure the production efficiency of K_α photons with high-energy (~Joule) prepulse levels. Results show a decrease in both K_α and bremsstrahlung yield with increasing artificial prepulse. Assuming energy contrast levels on the order of 10^{-5}, laser facilities such as the Advanced Radiography Capabilities (ARC) on NIF with estimated laser energies of 10kJ, it is important to understand the effects of joule level laser prepulses and how K_α production efficiency depends on it in the context of x-ray radiography. In this study, we see K_α yields reaching above $(1.0\pm0.2)\times10^{12}$ ph/sr or 3.3×10^{9} ph/sr per Joule of short pulse energy with minimal prepulse while dropping down to $(3.0\pm0.6)\times10^{11}$ ph/sr (1×10^{9} ph/sr/J) with the 5000mJ level prepulses. Simulations of the LPI show reduction of conversion efficiencies from 30% to 10% as the prepulse energy increases to the 5000mJ level, which accounts for the main reason that a reduction in K_α yield is observed. It can be seen that higher contrast laser systems will significantly improve the efficiency with which K_α is produced.

ACKNOWLEDGMENTS
This work was performed under the auspices of the U.S. Department of Energy by Lawrence Livermore National Laboratory under Contract DE-AC52-07NA27344

References

1) C. Stoeckl, J. A. Delettrez, R. Epstein, G. Fiksel, D. Guy, M. Hohenberger, R. K. Jungquist, C. Mileham, P. M. Nilson, T. C. Sangster, M. J. Shoup III, and W. Theobald. "Soft x-ray backlighting of direct-drive implosions using a spherical crystal imager on OMEGA." *Review of Scientific Instruments* 83.10 (2012): 10E501-10E501.
2) C. D. Chen, J. A. King, M. H. Key, K. U. Akli, F. N. Beg, H. Chen, R. R. Freeman, A. Link, A. J. Mackinnon, A. G. MacPhee, P. K. Patel, M. Porkolab, R. B. Stephens, and L. D. Van Woerkom. "A Bremsstrahlung spectrometer using< equation> k</equation>-edge and differential filters with image plate dosimeters." *Review of Scientific Instruments* 79.10 (2008): 10E305-10E305.
3) C. D. Chen, P. K. Patel, D. S. Hey, A. J. Mackinnon, M. H. Key, K. U. Akli, T. Bartal, F. N. Beg, S. Chawla, H. Chen, R. R. Freeman, D. P. Higginson, A. Link, T. Y. Ma, A. G. MacPhee, R. B. Stephens, L. D. Van Woerkom, B. Westover, and M. Porkolab.

"Bremsstrahlung and Kα fluorescence measurements for inferring conversion efficiencies into fast ignition relevant hot electrons." *Physics of Plasmas* 16 (2009): 082705.

4) K. T. Lorenz, M. J. Edwards, S. G. Glendinning, A. F. Jankowski, J. McNaney, S. M. Pollaine, and B. A. Remington. "Accessing ultrahigh-pressure, quasi-isentropic states of matter." *Physics of plasmas* 12.5 (2005): 056309-056309.
5) B.A. Remington, G. Bazan, J. Belak, E. Bringa, M. Caturla, J.D. Colvin, M.J. Edwards, S.G. Glendinning, D.S. Ivanov, B. Kad, D.H. Kalantar, M. Kumar, B.F. Lasinski, K.T. Lorenz, J.M. McNaney, D.D. Meyerhofer, M.A. Meyers, S.M. Pollaine, D. Rowley, M. Schneider, J.S. Stölken, J.S. Wark, S.V. Weber, W.G. Wolfer, B. Yaakobi, and L.V. Zhigilei. "Materials science under extreme conditions of pressure and strain rate." *Metallurgical and Materials Transactions A* 35.9 (2004): 2587-2607.
6) E. Brambrink, H. G. Wei, B. Barbrel, P. Audebert, A. Benuzzi-Mounaix, T. Boehly, T. Endo, C. D. Gregory, T. Kimura, R. Kodama, N. Ozaki, H.-S. Park, and M. Koenig. "Direct density measurement of shock-compressed iron using hard x rays generated by a short laser pulse." *Physical Review E* 80.5 (2009): 056407.
7) A G R Thomas, M Sherlock, C Kuranz, C P Ridgers and R P Drake. "Hybrid Vlasov–Fokker–Planck–Maxwell simulations of fast electron transport and the time dependance of K-shell excitation in a mid-Z metallic target." *New Journal of Physics* 15.1 (2013): 015017.
8) Z. Zhang, M. Nishikino, H. Nishimura, T. Kawachi, A. S. Pirozhkov, A. Sagisaka, S. Orimo, K. Ogura, A. Yogo, Y. Okano, S. Ohshima, A. Sunahara, S. Fujioka, H. Kiriyama, K. Kondo, T. Shimomura, and S. Kanazawa. "Efficient multi-keV x-ray generation from a high-Z target irradiated with a clean ultra-short laser pulse." *Optics Express* 19.5 (2011): 4560-4565.
9) H.-S. Park,D. M. Chambers, H.-K. Chung, R. J. Clarke, R. Eagleton, E. Giraldez, T. Goldsack, R. Heathcote, N. Izumi, M. H. Key, J. A. King, J. A. Koch, O. L. Landen, A. Nikroo, P. K. Patel, D. F. Price, B. A. Remington, H. F. Robey, R. A. Snavely, D. A. Steinman, R. B. Stephens, C. Stoeckl, M. Storm, M. Tabak, W. Theobald, R. P. J. Town, J. E. Wickersham, and B. B. Zhang. "High-energy Kα radiography using high-intensity, short-pulse lasers." *Physics of plasmas* 13 (2006): 056309.
10) H.-S. Park, B. R. Maddox, E. Giraldez, S. P. Hatchett, L. T. Hudson, N. Izumi, M. H. Key, S. Le Pape, A. J. MacKinnon, A. G. MacPhee, P. K. Patel, T. W. Phillips, B. A. Remington, J. F. Seely, R. Tommasini, R. Town, J. Workman, and E. Brambrink. "High-resolution 17–75 keV backlighters for high energy density experiments." *Physics of Plasmas* 15.7 (2008): 072705-072705.
11) B. Westover, A. MacPhee, C. Chen, D. Hey, T. Ma, B. Maddox, H.-S. Park, B. Remington, and F. N. Beg. "Study of silver Kα and bremsstrahlung radiation from short-pulse laser-matter interactions with applications for x-ray radiography." *Physics of Plasmas* 17 (2010): 082703.
12) W. Theobald, C. Stoeckl, P. A. Jaanimagi, P. M. Nilson, M. Storm, D. D. Meyerhofer, T. C. Sangster, D. Hey, A. J. MacKinnon, H.-S. Park, P. K. Patel, R. Shepherd, R. A. Snavely, M. H. Key, J. A. King, B. Zhang, R. B. Stephens, K. U. Akli, K. Highbarger, R. L. Daskalova, L. Van Woerkom, R. R. Freeman, J. S. Green, G. Gregori, K. Lancaster, and P. A. Norreys. "A dual-channel, curved-crystal spectrograph for petawatt laser, x-ray backlighter source studies." *Review of Scientific Instruments* 80.8 (2009): 083501-083501.
13) B. R. Maddox, H. S. Park, B. A. Remington, N. Izumi, S. Chen, C. Chen, G. Kimminau, Z. Ali, M. J. Haugh, and Q. Ma. "High-energy x-ray backlighter spectrum measurements using calibrated image plates." *Review of Scientific Instruments* 82.2 (2011): 023111-023111.

14) C.P.J. Barty, M. Key, J. Britten, R. Beach, G. Beer, C. Brown, S. Bryan, J. Caird, T. Carlson, J. Crane, J. Dawson, A.C. Erlandson, D. Fittinghoff, M. Hermann, C. Hoaglan, A. Iyer, L. Jones II, I. Jovanovic, A. Komashko, O. Landen, Z. Liao, W. Molander, S. Mitchell, E. Moses, N. Nielsen, H-H. Nguyen, J. Nissen, S. Payne, D. Pennington, L. Risinger, M. Rushford, K. Skulina, M. Spaeth, B. Stuart, G. Tietbohl and B. Wattellier. "An overview of LLNL high-energy short-pulse technology for advanced radiography of laser fusion experiments." *Nuclear Fusion* 44.12 (2004): S266.
15) John F. Seely, Glenn E. Holland, Lawrence T. Hudson, Csilla I. Szabo, Albert Henins, Hye-Sook Park, Prav K. Patel, Riccardo Tommasini, J. Martin Laming. "K-shell spectra from Ag, Sn, Sm, Ta, and Au generated by intense femtosecond laser pulses." *High Energy Density Physics* 3.1 (2007): 263-271.
16) J.F. Seely, R. Doron, A. Bar-Shalom, L.T. Hudson, C. Stoeckl. "Hard X-ray emission from laser-produced plasmas of U and Pb recorded by a transmission crystal spectrometer." *Journal of Quantitative Spectroscopy and Radiative Transfer* 81.1 (2003): 421-429.
17) B. R. Maddox, H. S. Park, B. A. Remington, and M. McKernan. "Calibration and characterization of single photon counting cameras for short-pulse laser experiments." *Review of Scientific Instruments*79.10 (2008): 10E924-10E924.
18) J. A. Halbleib, R. P. Kensek, T. A. Mehlhorn, G. D. Valdez, S. M. Seltzer, M. J. Berger. *ITS version 3.0: the integrated TIGER series of coupled electron/photon Monte Carlo transport codes*. Albuquerque, NM: Sandia National Laboratories, 1992.
19) Hui Chen, S. C. Wilks, W. L. Kruer, P. K. Patel, and R. Shepherd. "Hot electron energy distributions from ultraintense laser solid interactions." *Physics of plasmas* 16 (2009): 020705.
20) J. Myatt, W. Theobald, J. A. Delettrez, C. Stoeckl, M. Storm, T. C. Sangster, A. V. Maximov, and R. W. Short. "High-intensity laser interactions with mass-limited solid targets and implications for fast-ignition experiments on OMEGA EP." *Physics of plasmas* 14 (2007): 056301.
21) Y. Sentoku, T. E. Cowan, A. Kemp, and H. Ruhl. "High energy proton acceleration in interaction of short laser pulse with dense plasma target." *Physics of plasmas* 10 (2003): 2009.
22) A. G. MacPhee, L. Divol, A. J. Kemp, K. U. Akli, F. N. Beg, C. D. Chen, H. Chen, D. S. Hey, R. J. Fedosejevs, R. R. Freeman, M. Henesian, M. H. Key, S. Le Pape, A. Link, T. Ma, A. J. Mackinnon, V. M. Ovchinnikov, P. K. Patel, T. W. Phillips, R. B. Stephens, M. Tabak, R. Town, Y. Y. Tsui, L. D. Van Woerkom, M. S. Wei, and S. C. Wilks. "Limitation on prepulse level for cone-guided fast-ignition inertial confinement fusion." *Physical review letters* 104.5 (2010): 055002.
23) B. S. Paradkar, M. S. Wei, T. Yabuuchi, R. B. Stephens, M. G. Haines, S. I. Krasheninnikov, and F. N. Beg. "Numerical modeling of fast electron generation in the presence of preformed plasma in laser-matter interaction at relativistic intensities." *Physical Review E* 83.4 (2011): 046401.
24) T. Yabuuchi, B. S. Paradkar, M. S. Wei, J. A. King, F. N. Beg, R. B. Stephens, N. Nakanii, M. Hatakeyama, H. Habara, K. Mima, K. A. Tanaka, and J. T. Larsen. "Transport study of intense-laser-produced fast electrons in solid targets with a preplasma created by a long pulse laser." *Physics of Plasmas* 17 (2010): 060704.
25) M. M. Marinak, S. W. Haan, T. R. Dittrich, R. E. Tipton, and G. B. Zimmerman. "A comparison of three-dimensional multimode hydrodynamic instability growth on various

National Ignition Facility capsule designs with [small-caps HYDRA] simulations." *Physics of Plasmas* 5 (1998): 1125.

26) A. J. Kemp, B. I. Cohen, and L. Divol. "Integrated kinetic simulation of laser-plasma interactions, fast-electron generation, and transport in fast ignition."*Physics of Plasmas* 17 (2010): 056702.

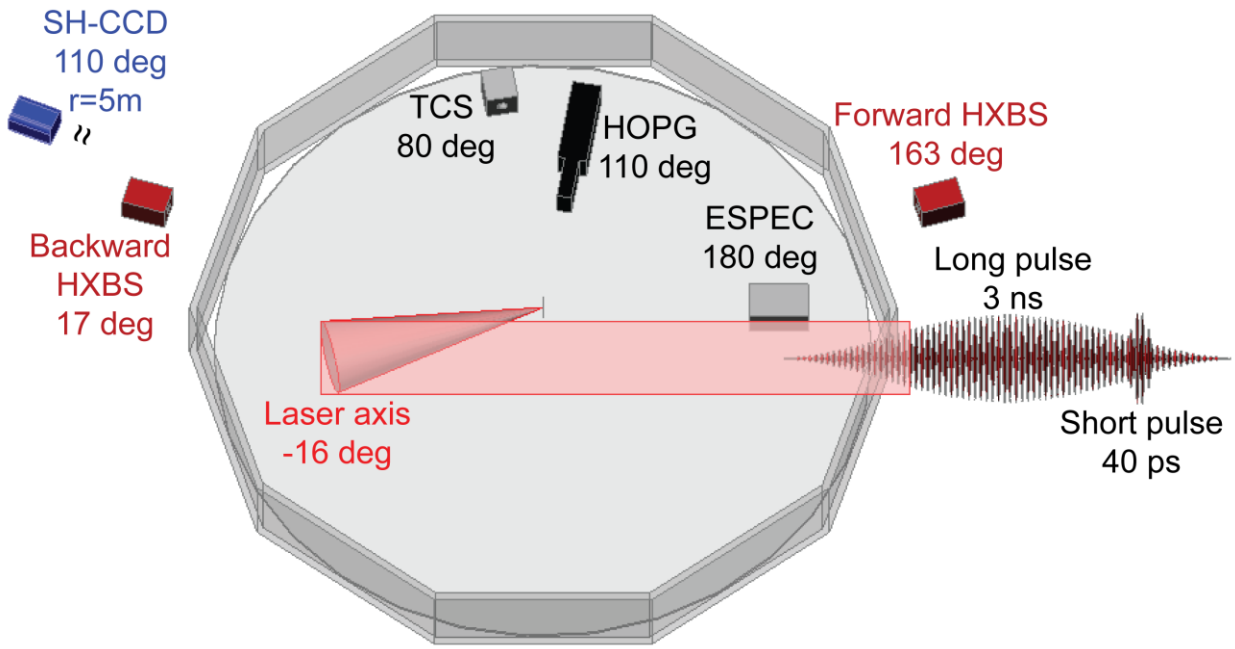

Figure 1: Schematic showing laser, target, and diagnostic layout geometries.

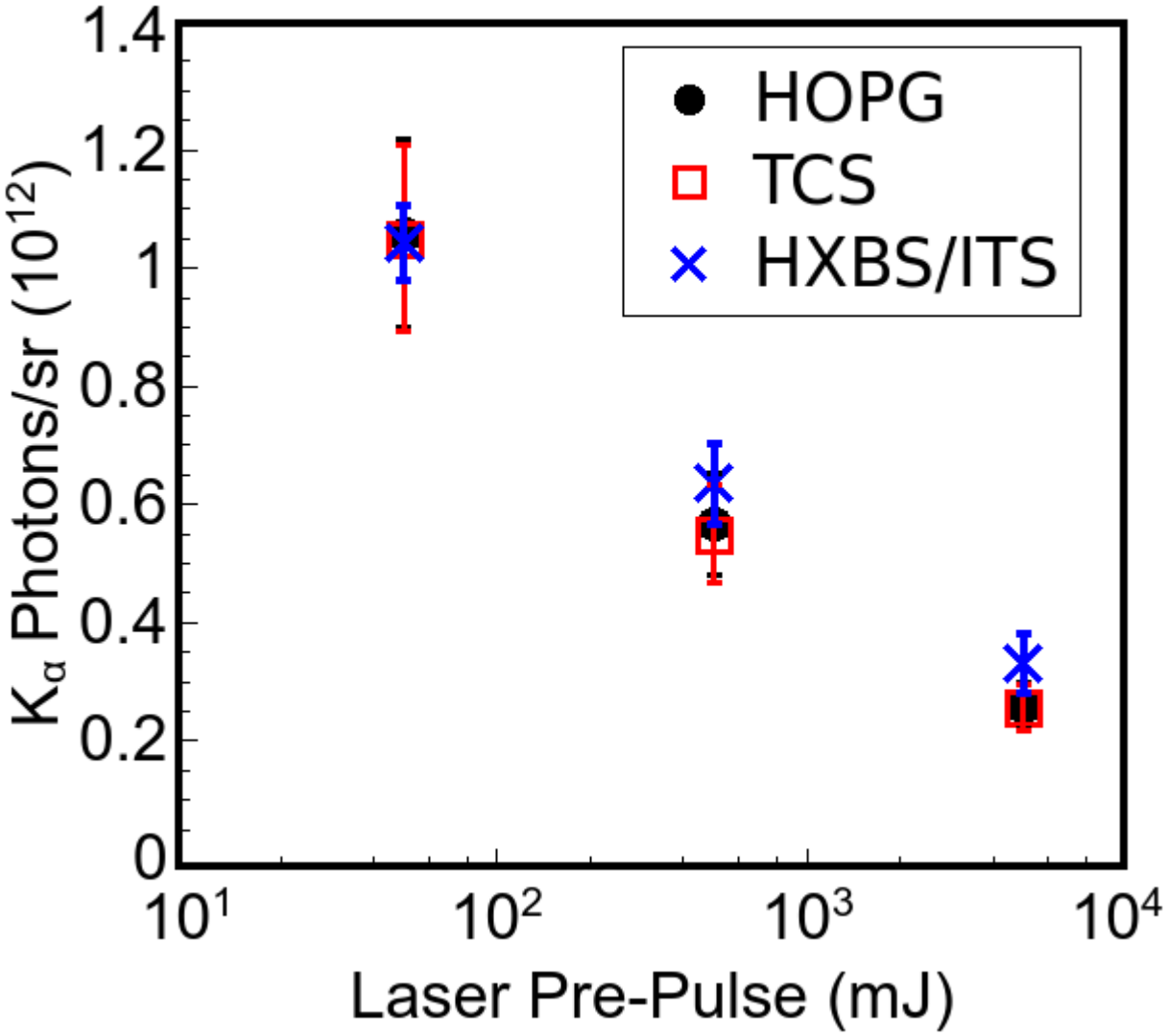

Figure 2: K_α yield as a function of artificially induced laser prepulse measured by HOPG and TCS as well as from the post-processing of the HXBS using ITS.

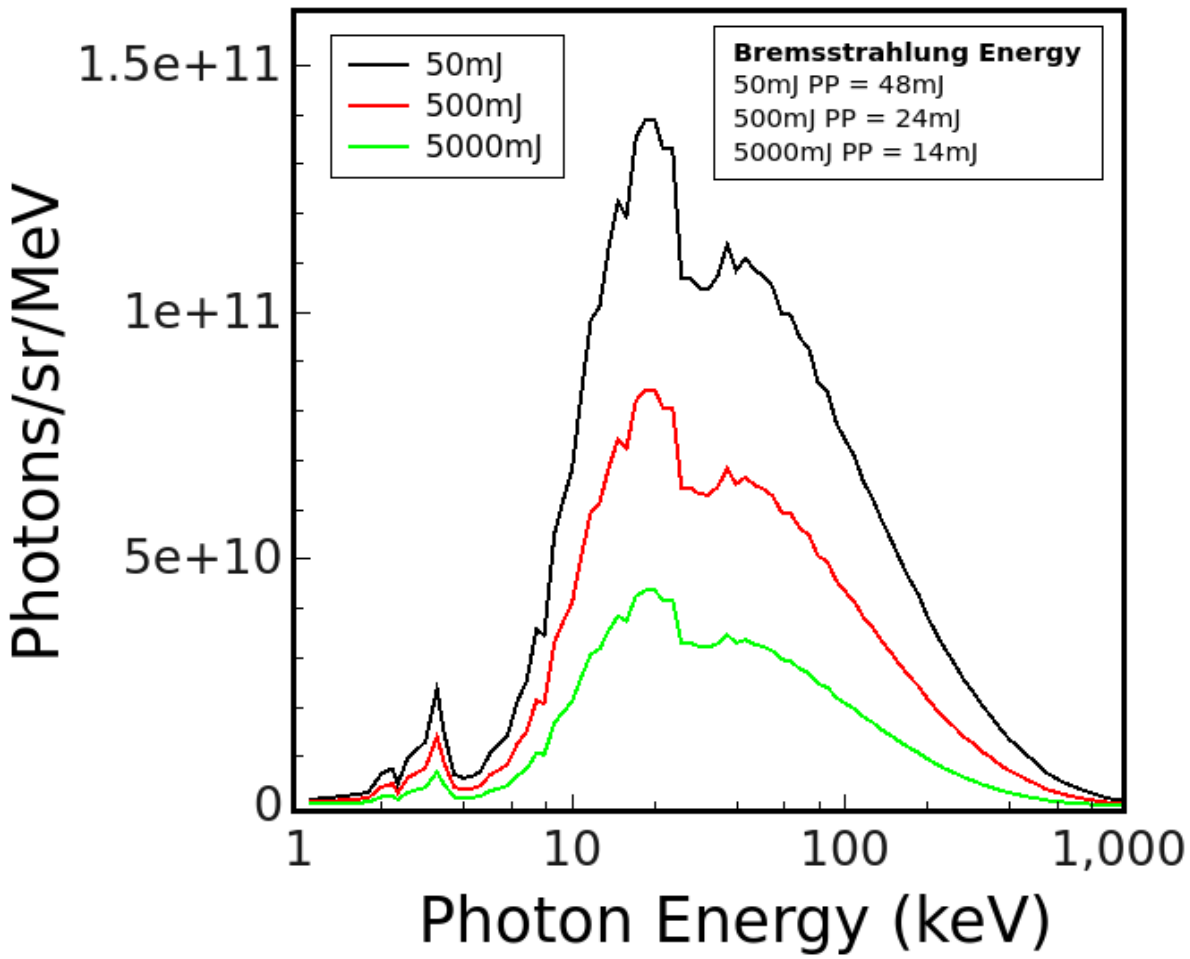

Figure 3: Bremsstrahlung spectra emitted from the target for three different prepulse energies obtained from the post-processing of the rear side HXBS using ITS. Total energy in the form of bremsstrahlung radiation decreases with increasing prepulse energy.

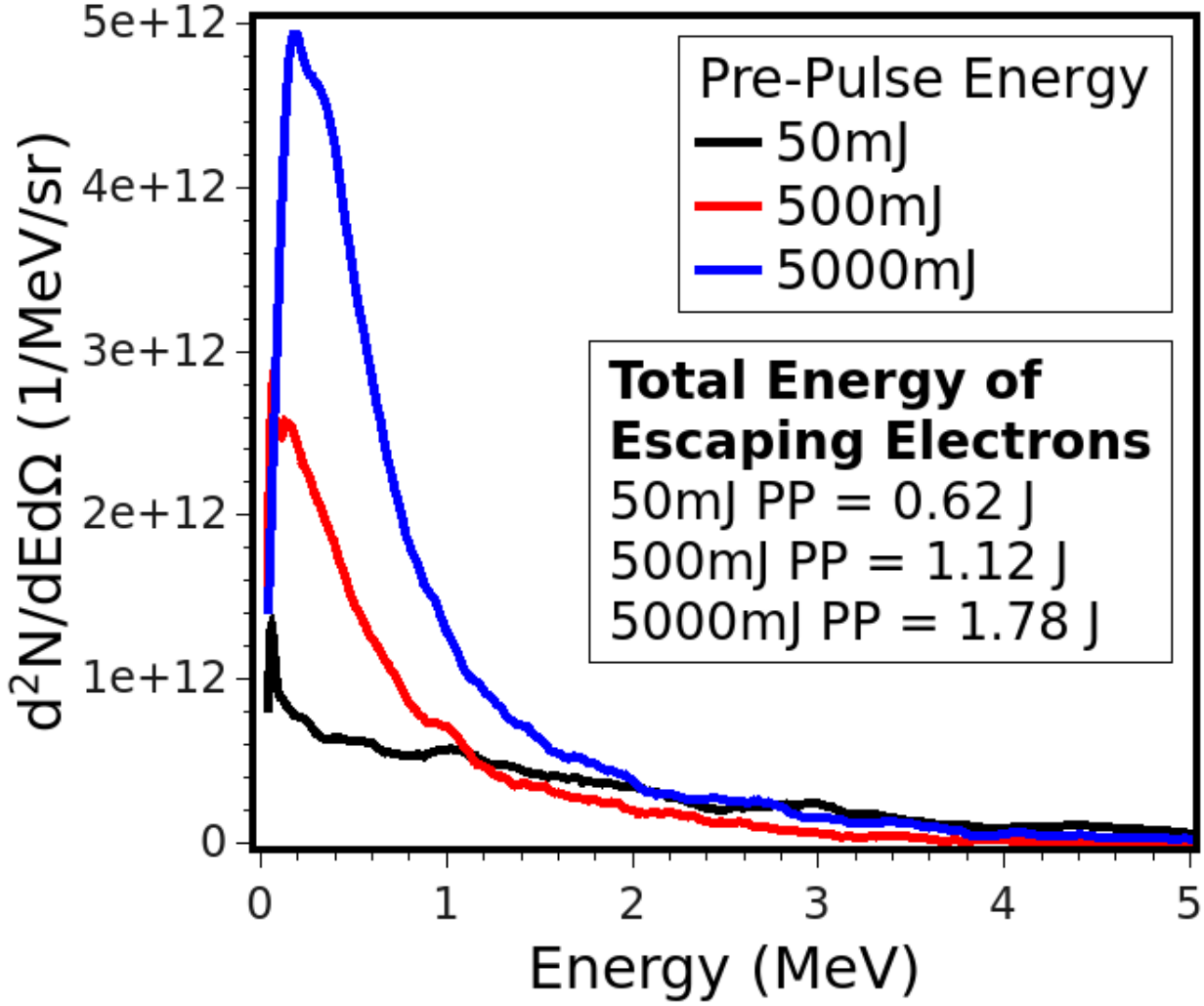

Figure 4: Vacuum electron spectra for three different prepulse energies obtained from the ESPEC. Total energy in the form of electrons escaping the target increases with increasing prepulse energy.

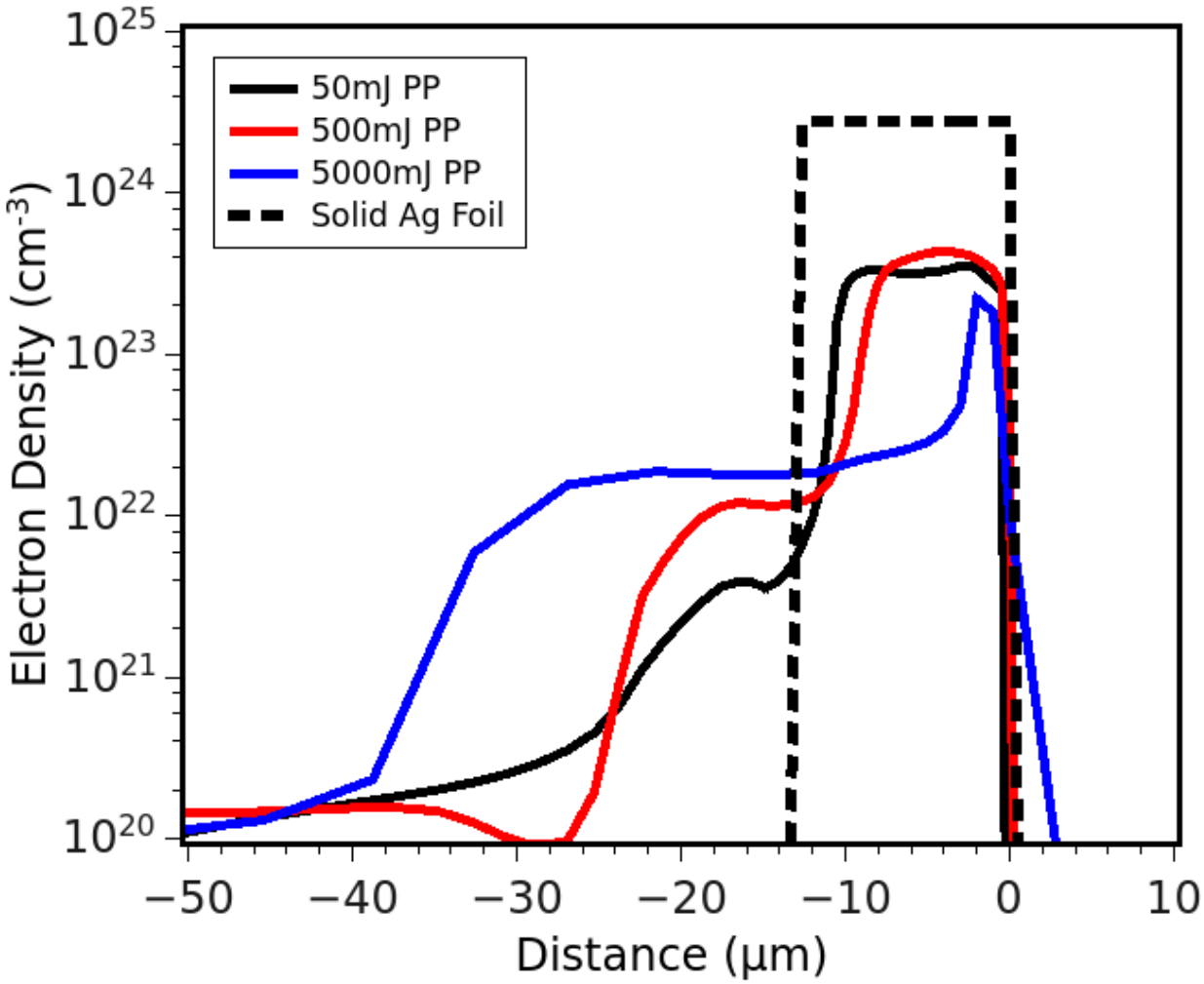

Figure 5: On-axis electron density profiles from HYDRA simulations for three different prepulse energies. The critical density for 1.053μm wavelength light gets pushed farther and farther back as the prepulse energy is increased.

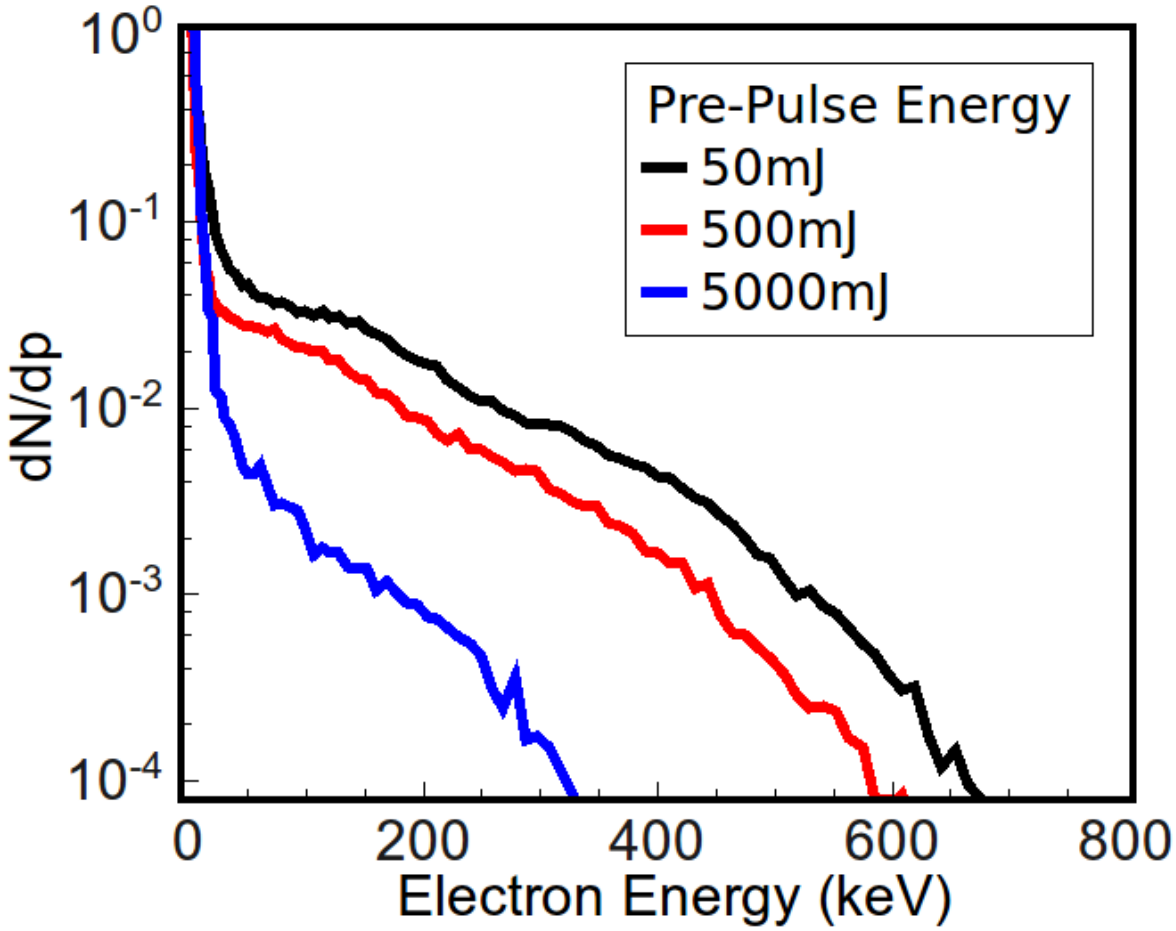

Figure 6: Electron source spectra from LPI simulations using PSC. Here the relative conversion efficiency of laser energy to fast electron energy decreases with increasing prepulse energy.

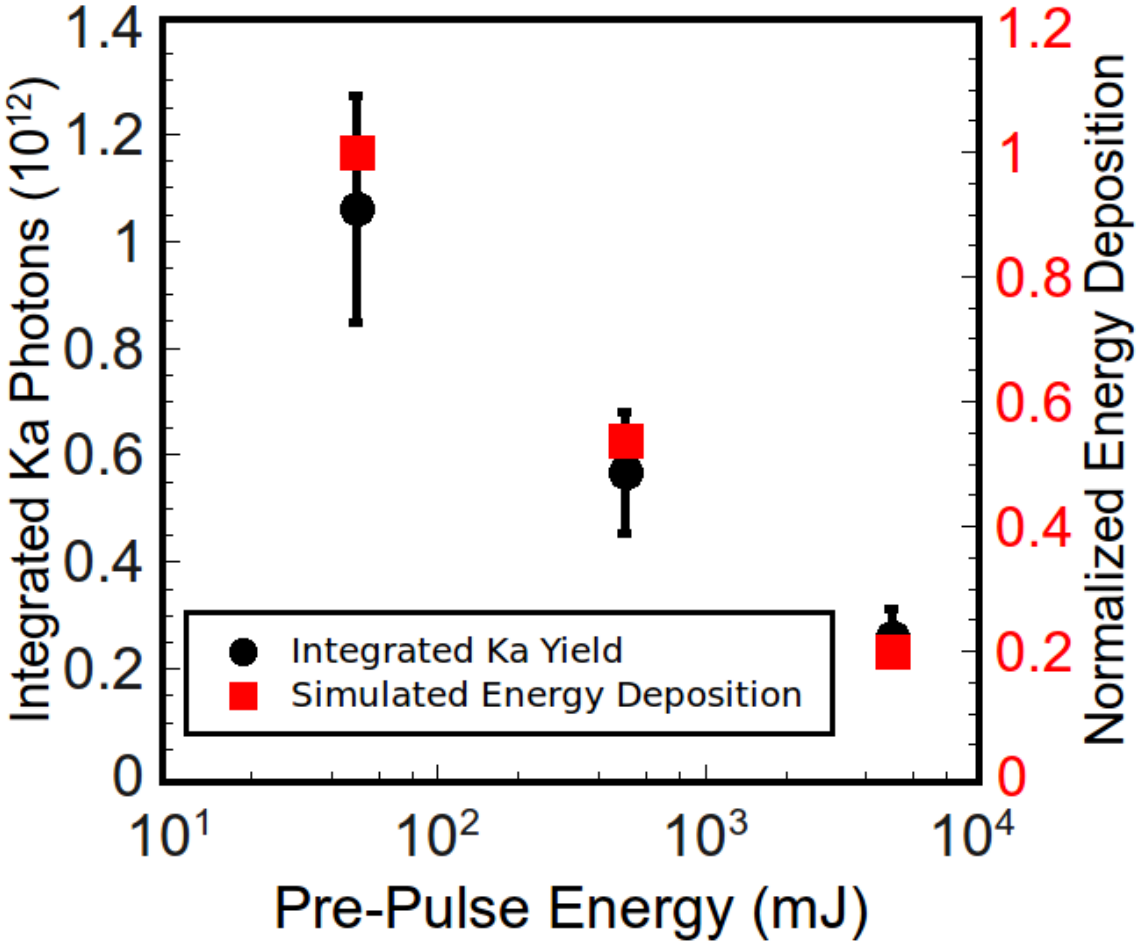

Figure 7: Relative comparison of K_α yield measured from the crystal spectrometers with the normalized energy deposition of fast electrons in a refluxing dominated regime.